GaN-on-Diamond Electronic Device Reliability: Mechanical and Thermo-Mechanical Integrity

Dong Liu,[1,2,a] Huarui Sun,[1] James W. Pomeroy,[1] Daniel Francis,[3] Firooz Faili,[3] Daniel J. Twitchen,[3] and Martin Kuball[1,b]

[1]*Center for Device Thermography and Reliability, H.H. Wills Physics Laboratory, University of Bristol, Bristol BS8 1TL, United Kingdom*

[2]*Interface Analysis Center, H.H. Wills Physics Laboratory, University of Bristol, Bristol BS8 1TL, United Kingdom*

[3]*Element-Six Technologies, Santa Clara, CA 95054, USA*

The mechanical and thermo-mechanical integrity of GaN-on-diamond wafers used for ultra-high power microwave electronic devices was studied using a micro-pillar based *in situ* mechanical testing approach combined with an optical investigation of the stress and heat transfer across interfaces. We find the GaN/diamond interface to be thermo-mechanically stable, illustrating the potential for this material for reliable GaN electronic devices.

AlGaN/GaN transistors have been transforming microwave applications ranging from communication to radar applications. Power densities as high as 40 W/mm have been demonstrated [1], and frequencies well exceeding 300 GHz [2]. Commercial applications, however, typically allow devices to operate only up to 5-7 W/mm, with the concern that excess device heating would result in early device failure. Usually AlGaN/GaN microwave devices are grown on SiC substrates; with their intrinsic high thermal conductivity of 450 W/mK, this enables relatively efficient heat extraction [3]. However, heat extraction is still the "Achilles heel" of current AlGaN/GaN electronic devices. Recently, the integration of AlGaN/GaN transistors with diamond substrates has been explored to reduce the device thermal resistance below current GaN-on-SiC devices. This has made it possible to triple the maximum possible power density that these microwave devices can deliver [4-6]. The active AlGaN/GaN part of the device used in this technology originates from a qualified epitaxy, as for example grown on Si substrates. Diamond is then used to replace the original substrate, either by diamond growth or by wafer-bonding [7-9]. Salient unknowns are the implications for device reliability considering the rather small thermal lattice expansion coefficient of the diamond compared with the GaN. Local debonding at the interface would lead to failure of the device. Accordingly, interfacial strengths in these devices represent an essential aspect that has to be evaluated and quantified prior to application. In this letter, we address this issue by adopting a unique *in situ* micro-scale mechanical testing approach. In conjunction with optical-based stress measurements and thermal boundary resistance measurements, we have found that GaN-on-diamond materials and device can have high thermo-mechanical stability, thus providing a fundamental basis towards a reliable device technology.

The GaN-on-diamond wafers studied comprised an AlGaN/GaN heterostructure grown on Si substrates by metal-organic chemical vapor deposition (MOCVD) as the starting material. Diamond with the thickness of ~100 μm was grown by

[a)] *Present address: Department of Materials, University of Oxford, Oxford OX1 3PH, United Kingdom*
[b)] *Authors to whom correspondence should be addressed. Electronic mail: Martin.Kuball@bristol.ac.uk*

microwave (MW) plasma CVD after removal of the Si substrate and the AlGaN strain relief layer. A 40 nm thin amorphous dielectric layer was used as a diamond seeding layer which was deposited onto the GaN by low-pressure CVD. Further details on the sample fabrication can be found in Ref. [9].

In terms of the evaluation of the strength of the GaN/diamond interface, a micro-scale testing approach was used. Micro-pillars comprising of the GaN, dielectric layer and diamond were created using focused Ga^+ beam milling in a FEI Helio NanoLab 600i Dualbeam workstation. The procedure for creating these micro-pillars is illustrated in Fig. 1a. Step I was to mill two parallel trenches (a voltage of 30 kV and current of 6.5 nA was used) along a 45° angle into the cross-section of GaN-on-diamond wafer; step II involved turning the wafer through 180 degrees to allow the removal of another two parallel trenches with a 90° angle from the previous direction. On the completion of these two steps, a cross-section cleaning mode was used to clean the four surfaces of the pillar using a low current - typically 96 pA to remove Ga^+ implanted layer, followed by a final step of cleaning the edge of the GaN layer by applying a 30 kV/48 pA current. A customized piezoelectric force measurement Si probe with a micromanipulator (Kleindiek Nanotechnik, Germany) was used to apply load to the GaN layer with a precision of 0.1 μN (maximum load = 360 μN). The displacement and the fracture process could be viewed continuously in a scanning electron microscope (SEM). As indicated in Fig. 1a, the micro-pillar was titled 45° to allow mechanical load to be applied from above the GaN layer to create a stress at the GaN/diamond interface. Further details on this micro-mechanical testing technique can be found in Ref. [11,12].

Raman spectroscopy measurements were performed on the samples heated to different temperatures, in a nitrogen atmosphere, to evaluate the stress state of the GaN layer. A Renishaw InVia confocal Raman microscope with a 488 nm laser was used, with a laser spot size of 1 μm [13]. The thermal resistance of the interface between the GaN and the diamond was determined by transient thermoreflectance. A 355 nm frequency-tripled Nd:YAG laser (3.49 eV, *i.e.*, above GaN bandgap) with a pulse duration of 10 ns was used as a heating pulse to induce a rapid temperature rise at the surface of the AlGaN/GaN. The change in surface reflectance was monitored by a continuous wave (CW), 532 nm frequency-doubled Nd:YAG laser to track the temperature rise, from which thermal boundary resistance (TBR_{eff}) of the GaN/diamond interface could be determined. Further details on this technique are published elsewhere [9,14].

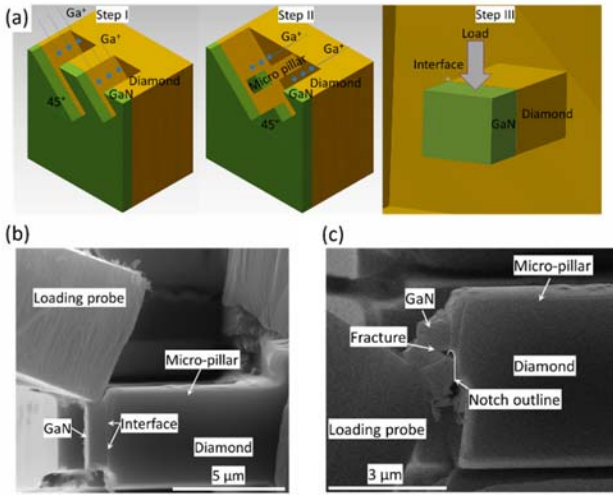

Fig. 1. (a) Schematic of the fabrication steps for the GaN-on-diamond micro-pillars; (b) a typical GaN-on-diamond micro-pillar with the load applied by a Si probe onto the GaN layer; (c) fracture occurred through the thickness of the GaN at 300 μN while the interface remained intact.

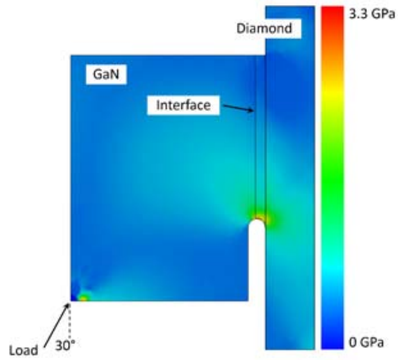

Fig. 2. Finite element simulation of the maximum principal stress distribution in the GaN-on-diamond micro-pillar around the notch, at a load of 300 μN. For clarity, only the crucial region around the notch tip is displayed.

To test the mechanical stability of the GaN/diamond interface, different sizes of micro-pillars were created; a typical pillar is shown in Fig. 1b. Each pillar consists of two parts: the base diamond pillar with the size of 4 × 4 × 7 μm and the top GaN layer with a smaller section to allow well-controlled loading, *e.g.*, with a size of 3 × 3 × 0.8 μm (Figure 1b). A load was applied parallel to the interface on the GaN layer to create a stress to cause the interface to fail. However, the maximum load of 360 μN generated by the probe was not sufficient to exceed the strength of the interface. The size of the GaN layer was therefore subsequently reduced to 0.7 × 3 μm and a stress raiser / concentrator, specifically a sharp notch diameter 70 nm, at the interface was created by line milling at a Ga^+ current of 26 pA. Figure 1c shows the original outline of the notch. With this geometry, a load of 300 μN was reached prior to the fracture of the GaN. It is evident from SEM imaging that the fracture occurred at the tip of the notch, but it propagated through the thickness of the GaN along a cleavage plane while the GaN/diamond interface remained undamaged (Figure 1c). To further quantify the stress level created in the loading process, a finite element-based multi-layer numerical model was performed using material parameters listed in Table I. The full geometry of the micro-pillar and the loading process was simulated. A load of 300 μN was applied at the top corner of the GaN layer at an angle of 30^0 to the GaN surface as in the experimental configuration. Adaptive mesh refinement was used to achieve a convergent result at the notch tip. For brittle materials studied, the primary failure criteria will be one of the maximum tangential stresses, i.e., the maximum principal stress, which would yield an opening mode fracture or maximum dissipated energy path. Therefore, distribution of the maximum principal stress around the notch tip prior to failure was plotted in Fig. 2 indicating that the failure stress was about 3.3 GPa. This provides a lower bound to the strength of the GaN/diamond interface, and implies that the stress required to delaminate GaN from the diamond structure will be higher than this value.

Table I Input parameters for the finite element analysis model [15-17]

	Young's modulus (GPa)	Poisson's ratio
Diamond	105	0.100
GaN	181	0.352
Dielectric layer	160	0.253

Due to the thermal expansion mismatch between the GaN and diamond, stresses are introduced into the GaN layer by changes in temperature that a device would encounter during processing or operation. If the induced thermal stresses exceed the interface strength, then there is a clear potential for device failure. Therefore, *in situ* quantification of these thermal stresses was undertaken using Raman spectroscopy when the sample was heated to various temperatures; results are shown in Fig. 3. The biaxial stress was determined using the E_2 GaN Raman peak considering a stress coefficient of 2.7 cm^{-1}/GPa [18]; the temperature contribution to the measured phonon frequency shift was subtracted, by comparing to a calibration performed on a stress-free bulk GaN wafer. At room temperature, there is a compressive stress of 0.35 GPa, which increases to 1.5 GPa at 900°C, *i.e.,* higher than typical diamond growth temperatures. This compressive stress is due to the thermal lattice expansion coefficient mismatch between diamond and GaN, which is in the 10^{-6} K^{-1} range. It should be noted that this stress is therefore significantly smaller than the stress needed to break the GaN layer (or the GaN/diamond interface) in our micro-pillar mechanical tests.

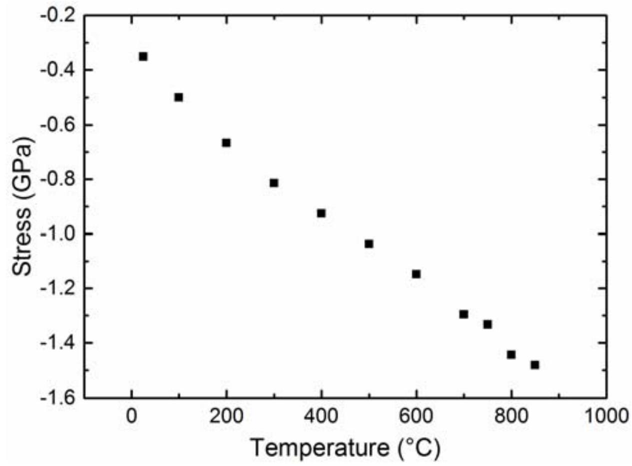

Fig. 3. Stress in the GaN layer on the GaN-on-diamond sample as function of temperature. Negative sign indicates compressive stress.

During the thermal treatment, the TBR_{eff} between the GaN and diamond was monitored in a sample area with no apparent defects. Each sample had been annealed for 10 mins in nitrogen at a different temperature, and the change in TBR_{eff} is plotted in Fig. 4. It was found that the TBR_{eff} remained constant, within scatter, as a function of annealing temperature, which confirmed the mechanical stability of the GaN-on-diamond material system for the interface studied. This strongly implies that the mismatch stresses introduced by thermal annealing do not cause significant interfacial damage. This is a very important finding because the primary concern that thermo-mechanical stress may result in premature failure of GaN-on-diamond electronic devices can therefore be excluded, for the materials studied here.

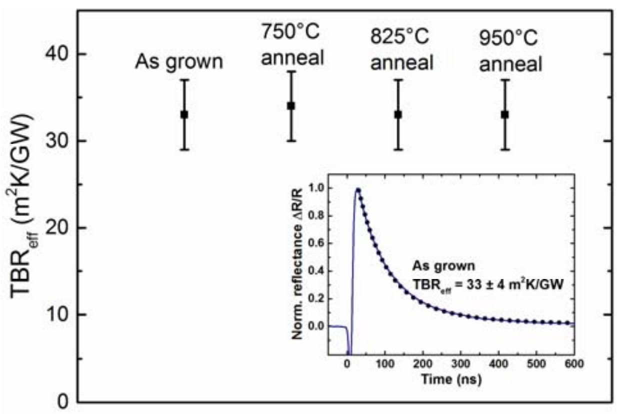

Fig. 4. Thermal boundary resistance (TBR_{eff}) of the GaN/diamond interface of as-grown sample and after annealing, measured at room temperature. Inset displays the thermo-reflectance transient to extract TBR_{eff}.

In conclusion, an *in situ* micro-pillar testing approach has been applied to GaN-on-diamond wafers to investigate the structural integrity of its dissimilar-material interfaces. The results demonstrate a high mechanical stability of the GaN/diamond interface studied showing the potential of this material system for reliable devices.

Acknowledgement

This work is in part supported by DARPA under Contract No: FA8650-15-C-7517 monitored by Dr. Avram Bar Cohen, supported by Dr. John Blevins, Dr. Joseph Maurer and Dr. Abirami Sivananthan. Any opinions, findings, and conclusions or recommendations expressed in this material are those of the authors and do not necessarily reflect the views of DARPA. DL acknowledges the financial support from the Royal Commission for the Exhibition of 1851. The authors thank Prof. Robert Ritchie (UC Berkeley, USA) for valuable discussions.

[1] Y. F. Wu, M. Moore, A. Saxler, T. Wisleder, and P. Parikh, in Proc. 64th DRC Tech. Dig., pp. 151–152, 2006,

[2] K. Shinohara, D.C. Regan, Y. Tang, A.L. Corrion, D.F. Brown, J.C. Wong, J.F. Robinson, H.H. Fung, A. Schmitz, T.C. Oh, S.J. Kim, P.S. Chen, R.G. Nagele, A.D. Margomenos, and M. Micovic, IEEE Trans. Electron Dev. **60**, 2982 (2013).

[3] A. Manoi, J.W. Pomeroy, N. Killat, and M. Kuball, IEEE Electron Device Lett. **31**, 1395 (2010).

[4] D. C. Dumka, T. M. Chou, F. Faili, D. Francis, and F. Ejeckam, Electron. Lett. **49**, 1298 (2013).

[5] J. W. Pomeroy, M. Bernardoni, D. C. Dumka, D. M. Fanning, and M. Kuball, Appl. Phys. Lett. **104**, 083513, (2014).

[6] J.D. Blevins, G.D. Via, K. Chabak, A. Bar-Cohen, J. Maurer, A. Kane, in Proc. CS MANTECH Conf., pp. 105–108, 2014.

[7] D. Francis, F. Faili, D. Babić, F. Ejeckam, A. Nurmikko and H. Maris, Diamond Rel. Mater. **19**, 229 (2010).

[8] P.C. Chao, Kanin Chu and Carlton Creamer, "A New High Power GaN-on-Diamond HEMT with Low-Temperature Bonded Substrate Technology," in Proc. CS Mantech Conf., pp. 179–182, 2013.

[9] H. Sun, R.B. Simon, J.W. Pomeroy, D. Francis, F. Faili, D.J. Twitchen, and M. Kuball, Appl. Phys. Lett. **106**, 111906 (2015).

[10] M. Faqir, T. Batten, T. Mrotzek, S. Knippscheer, M. Massiot, L. Letteron, S. Rochette, O. Vendier, J. M. Desmarres, F. Courtade, and M. Kuball, in Proc. of 27th IEEE SEMI-THERM Symposium, pp. 314–316, 2011.

[11] D. Liu, P. J. Heard, S. Nakhodchi and P. E. J. Flewitt, "Small-Scale Approaches to Evaluate the Mechanical Properties of Quasi-Brittle Reactor Core Graphite," in Graphite Testing for Nuclear Applications, ASTM (International), pp. 1-21, 2014.

[12] D. Liu, P. J. Heard, P. E. J. Flewitt and D. J. Smith, Key. Eng. Mater., **627**, 53 (2015).

[13] M. Kuball, Surf. Interface Anal. **31**, 987 (2001).

[14] J. W. Pomeroy, R. B. Simon, H. Sun, D. Francis, F. Faili, D. J. Twitchen, and M. Kuball, IEEE Electron Device Lett. **35**, 1007 (2014).

[15] http://www.ioffe.ru/SVA/NSM/

[16] T. Kramer, and O. Paul, in Proceedings of IEEE Sixteenth Annual International Conference on Micro Electro Mechanical Systems, pp. 678-81, 2003.

[17] V. Ziebart, O. Paul, U. Munch, and H. Baltes, in Proceedings of Materials Research Society Symposium, vol. 505, pp. 27-32, 1998.

[18] J.M. Wagner and F. Bechstedt, Phys. Stat. Sol. (b) **234**, 965 (2002).